Focused Ion Beam Production Using a Pyroelectric Crystal and a Resistive Glass Tube

T. Z. Fullem, A. M. Kovanen, D. J. Gillich, and Y. Danon

Abstract– **We describe the use of a lithium tantalate ($LiTaO_3$) pyroelectric crystal and a resistive glass tube to generate a focused ion beam. A sharp tip was mounted on one surface of the $LiTaO_3$ crystal which ionized a low pressure deuterium gas. A resistive glass tube was mounted coaxially with the tip. The resultant ion beam produced an illuminated spot on a ZnS screen. Experimental results were compared with finite element modeling performed using COMSOL Multiphysics. It was found that the spot size increased as the distance between the screen and the end of the resistive glass tube increased, which agreed with the COMSOL model.**

I. Introduction

PYROELECTRIC materials exhibit a nonzero spontaneous polarization under equilibrium conditions and this polarization is a function of the material's temperature [1]. When a pyroelectric crystal experiences a change in temperature, the polarization also changes and results in an electric field that is strong enough to accelerate charged particles to energies [2] on the order of 100 keV. Equations for calculating the potential and field in pyroelectric accelerators are available in the literature [3]. The use of pyroelectric accelerators to accelerate electrons into a metal target has led to the production of compact X-Ray generators [4], [5], [6]. By affixing a sharp tip to one surface of the crystal, the electric field in the vicinity of the tip is increased which allows for enhanced field ionization of the surrounding gas [7], [8]. If deuterium ions produced thusly are accelerated into a deuterated target, D–D nuclear fusion occurs and can be utilized as a neutron source [7], [8], [9], [10]. Arrays of nanostructures have also been used to enhance ionization [11], [12]. Other investigators have reported various techniques for producing focused electron beams in pyroelectric accelerators [13], [14], [15]. We report here the use of a resistive glass tube in a pyroelectric accelerator to form a focused ion beam.

II. Experimental Methods

The pyroelectric material used in the experiments discussed herein was a cylindrical lithium tantalate ($LiTaO_3$) crystal, cut such that the cylinder's axis was parallel to the axis of polarization. The crystal had a radius of 1 cm and a thickness of 1 cm. A Cu disk with a radius of 4.5 mm was affixed to the center of one face of the crystal using Ag filled epoxy. A standard DIP socket was soldered to the center of the disk, and sharp tungsten tip (marketed for use in a scanning electron microscope) with an apex radius of 70 nm was mounted in the socket. A resistive glass tube with an inner radius of 5.2 mm, a wall thickness of 1.8 mm, and a length of 2 cm was attached to the same surface of the crystal using Ag filled epoxy such that it was coaxial with the tip, Cu disk and crystal. The other surface of the crystal was electrically grounded and attached to a thermoelectric cooler (TEC) to facilitate heating and cooling the crystal. The tip was pointed at a ZnS screen which produces visible light when charged particles collide with it. A digital camera was mounted behind the screen to record the light that resulted from the ion beam. The experimental setup is shown in Fig. 1 and was mounted inside a vacuum chamber such that the crystal could be moved in a linear fashion allowing for easy adjustment of the separation distance between the end of the tube and the screen. The back of the TEC was mounted on an Al block which served as a heatsink and was attached to an Al rod which provided mechanical connection to the linear motion system. The walls of the vacuum chamber were stainless steel and electrically grounded. The distance between the screen and the camera was fixed. A photograph of the resistive glass tube, pyroelectric crystal, TEC, and the Al block assembly is shown in Fig. 2. A thermocouple was attached to the surface of the TEC which was in contact with the crystal, so that the temperature could be measured.

The crystal was heated from room temperature to 100°C in a ~2.5 mTorr deuterium atmosphere and allowed to cool naturally. During cooling, the crystal surface on which the tip was affixed became positively charged. The surrounding deuterium gas was ionized and these ions were accelerated away from the crystal and impacted the ZnS screen. Digital photographs of the ZnS screen were obtained at regular intervals while the crystal was cooling. Electrons were also accelerated toward the positively charged crystal face and the energy spectrum of the resultant X-Rays was measured; the maximum X-Ray energy is indicative of the ion energy.

Resistive glass is a commercially available glass whose surface has been doped such that it has a high resistivity lower than that of normal glass [16]. The resistive glass tube was attached to the face of the pyroelectric crystal using an electrically conductive Ag filled epoxy. When the face of the pyroelectric crystal was at a high potential, the resistive glass

Manuscript received November 12, 2009. This work was supported by the U. S. Department of Homeland Security under cooperative agreement number 2007-DN-077-ER0003.

The authors are with the Department of Mechanical, Aerospace and Nuclear Engineering, Rensselaer Polytechnic Institute, Troy, NY.

A. M. Kovanen and D. J. Gillich are also with the Department of Physics, United States Military Academy, West Point, NY.

(e-mail: danony@rpi.edu).

tube was also at an elevated potential due to its non-negligible (albeit low) electrical conductivity. As a result ions were repelled from the resistive glass tube. Since the ions were created along the axis of the tube, this repulsion focused the ions that were traveling toward the opening of the tube.

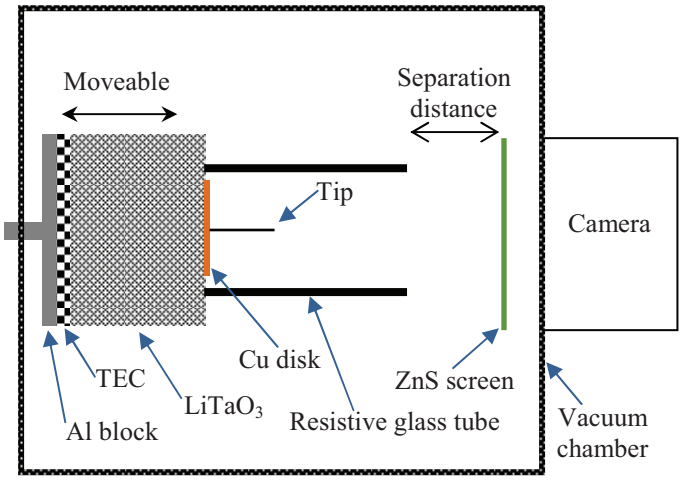

Fig. 1. Experimental setup.

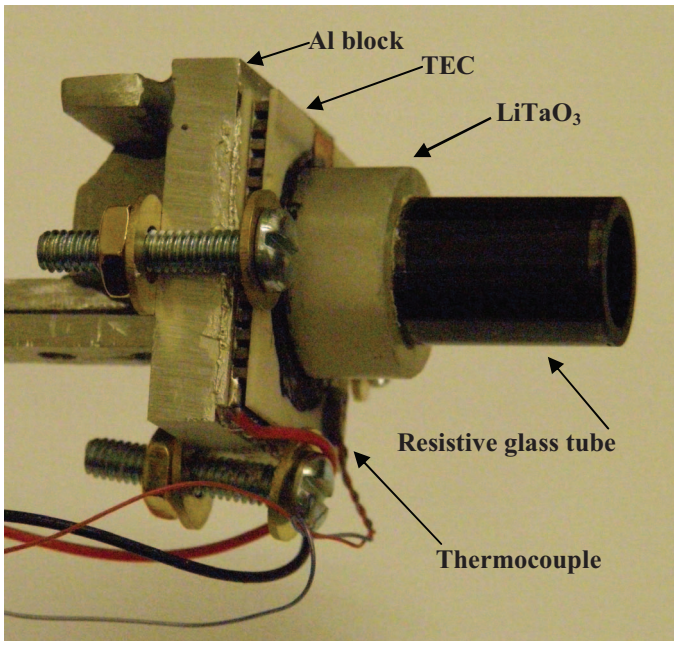

Fig. 2. Photograph of the pyroelectric crystal with a resistive glass tube on one face and a thermoelectric cooler (TEC) on the other face. The Al block serves as a heatsink for the TEC and is connected to the linear motion system.

III. Finite Element Modeling

Finite element modeling was performed with COMSOL Multiphysics 3.5a. The experimental setup shown in Fig. 1 was represented in COMSOL using the axial-symmetric geometry shown in Fig. 3a. This was used to calculate the electric potential and field throughout the system. The particle tracing feature in COMSOL was used to determine the paths that deuterium ions would follow as a result of being subjected to the calculated potential and field. The results of the COMSOL calculations are shown in Fig. 3b. The potentials were calculated and their spatial distribution is indicated by the shade of the grey background where a lighter shade indicates a higher potential; the calculated potentials range from 0 to 100 kV. The calculated ion tracks are indicated by the green lines in the figure. It should be noted that COMSOL was operated in a mode in which only electromagnetic calculations were performed, and therefore the fact that the ions were unable to penetrate the glass tube was not included in the calculation. Therefore the ion tracks shown in Fig. 3b which penetrate the tube and spread out to the side are not physical. Based on the calculated ions tracks which emanate from the opening of the tube, it can be predicted that the ions will form a focused spot and that the diameter of the spot increases with increasing distance from the end of the tube. In the absence of the tube, the COMSOL calculations indicate that the ions will spread out uniformly from the tip (covering a solid angle of 2π sr directed away from the crystal); this differs from the sketch in [10].

IV. Results

The procedure described above was conducted three times at each of four different separation distances. During each of these cooling cycles a focused ion beam was produced resulting in a glowing spot on the ZnS screen. Multiple images were collected during each cooling cycle. An example image is shown in Fig. 4a. A simple image analysis was conducted on several images from each cooling cycle so that the spot size could be determined. For each column in a given image, the sum of all of the pixels in that column was calculated. In Fig. 4b we see a plot showing the column number on the abscissa and the value of the sum of the pixels on the ordinate. Columns which contain bright regions have a larger sum than columns than columns that do not; the peak in Fig. 4b corresponds to the bright spot in Fig. 4a. The peak width, and therefore spot diameter, was calculated by performing a Gaussian fit of the peak; such a fit is shown in Fig. 4b. A dark image was obtained at a time when the system was not producing ions and was subtracted from all images prior to analysis to account for camera anomalies such as hot pixels.

Spot size versus the tube-screen separation distance was plotted in Fig. 4c and it was found that the spot size increased with increased separation distance. The error bars shown on the plot correspond to the uncertainties in the spot widths calculated by the Gaussian fit. This indicates that the ion beam's diameter increases as it travels away from the end of the tube. Finite element modeling of the ion trajectories calculated in COMSOL Multiphysics agrees with this result as shown in Fig. 3b.

During these experiments X-Rays were also produced. The X-Ray energy spectrum was measured and it was found that the X-Ray endpoint energy was 70 keV; this is indicative of the ion energy. An experiment was also conducted without the ZnS screen installed and no spot was observed. This verifies that when a spot was observed (c.f. Fig. 4a) it was due

to the glowing screen and not a plasma glow near the tip. With the screen removed, images of the crystal (with a radius of 1 cm) were obtained at several different crystal positions and these images were used to calibrate the size of the images. It was found that at the position of the screen, there were 0.2 mm/pixel.

(a)

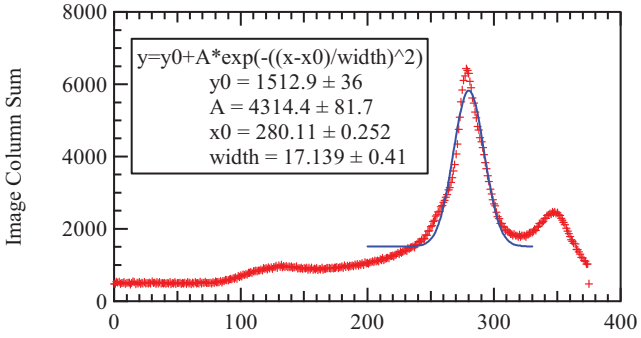

(b)

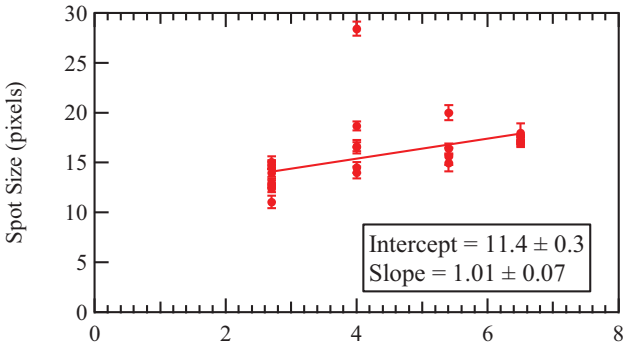

(c)

Fig. 4. (a) Photograph of the spot produced by the ion beam on the ZnS screen. (b) Determination of spot width using a Gaussian fit of the sums of the pixels in each column. (c) Spot width observed in multiple experiments conducted at four different tube-screen separation distances. It should be noted that 1 pixel corresponds to 0.2 mm.

V. Conclusions

We have described experiments in which a pyroelectric crystal with a sharp tip mounted on its surface was used to ionize low pressure deuterium gas and a resistive glass tube (which was also mounted on the surface of the crystal) was used to redirect these ions so as to form a focused spot. It was found that the spot size increased with increased distance from the end of the tube. The maximum energy of the ions was approximately 70 keV.

References

[1] S. B. Lang, "Pyroelectricity: From Ancient Curiosity to Modern Imaging Tool," *Phys. Today*, pp. 31-36, Aug., 2005.

[2] J. A. Geuther, Y. Danon, "High-energy x-ray production with pyroelectric crystals," *J. Appl. Phys.*, vol. 97, no. 10, 104916, 2005.

[3] T. Z. Fullem, Y. Danon, "Electrostatics of pyroelectric accelerators," *J. Appl. Phys.*, vol. 106, no. 7, 074101, 2009.

[4] J. D. Brownridge, "Pyroelectric X-ray generator," *Nature*, vol. 358, pp. 287-288, July 1992.

[5] J. D. Brownridge and S. Raboy, "Investigations of pyroelectric generation of x rays," *J. Appl. Phys.*, vol. 86, no. 1, pp. 640-647, 1999.

[6] J. D. Brownridge and S. M. Shafroth, "X-ray fluoresced high-Z (up to Z=82) K x rays produced by $LiNbO_3$ and $LiTaO_3$ pyroelectric crystal electron accelerators," *Appl. Phys. Lett.*, vol. 85, no. 7, pp. 1298-1300, 2004.

[7] J. Geuther, Y. Danon, F. Saglime, "Nuclear Reactions Induced by a Pyroelectric Accelerator," *Phys. Rev. Lett.*, vol. 96, 054803, 2006.

[8] D. Gillich, A. Kovanen, B. Herman, T. Fullem, Y. Danon, "Pyroelectric crystal neutron production in a portable prototype vacuum system," *Nucl. Instrum. Methods A*, vol. 602, no. 2, pp. 306-310, 2009.

[9] B. Naranjo, J. K. Gimzewski, and S. Putterman, "Observation of nuclear fusion driven by a pyroelectric crystal," *Nature*, vol. 434, pp. 1115-1117, April 2005.

[10] V. Tang, J. Morse, G. Meyer, S. Falabella, G. Guethlein, P. Kerr, H. G. Park, B. Rusnak, S. Sampayan, G. Schmid, C. Spadaccini, and L. Wang, "Crystal Driven Neutron Source: A New Paradigm for Miniature Neutron Sources," *20th Int. Conf. on Application of Accelerators in Research and Industry*, AIP Conf. Proc. vol. 1099, pp. 870-873, 2009.

[11] D. J. Gillich, R. Teki, T. Z. Fullem, A. Kovanen, E. Blain, D. B. Chrisey, T. –M. Lu, and Y. Danon, "Enhanced pyroelectric crystal D–D nuclear fusion using tungsten nanorods," *Nano Today*, vol. 4, no. 3, pp. 227-234, 2009.

[12] R. L. Fink, N. Jiang, L. Thuesen, K. N. Leung, A. J. Antolak, "Carbon Nanotube Based Deuterium Ion Source for Improved Neutron Generators," *20th Int. Conf. on Application of Accelerators in Research and Industry*, AIP Conf. Proc. vol. 1099, pp. 610-613, 2009.

[13] J. D. Brownridge, and S. M. Shafroth, "Pressure dependence of energetic (≤160 keV) focused electron beams arising from heated or cooled ($LiNbO_3$) pyroelectric crystals," *Appl. Phys. Lett.*, vol. 83, no. 7, pp. 1477-1479, 2003.

[14] N. Kukhtarev, J. D. T. Kukhtareva, M. Bayssie, J. Wang, J. D. Brownridge, "Generation of focused electron beam by pyroelectric and photogalvanic crystals," *J. Appl. Phys.*, vol. 96, no. 11, pp. 6794-6798, 2004.

[15] J. D. Brownridge and S. M. Shafroth, "Self-focused electron beams produced by pyroelectric crystals on heating or cooling in dilute gases," *Appl. Phys. Lett.*, vol. 79, no. 20, pp. 3364-3366, 2001.

[16] Burle Industries, Inc., http://www.burle.com.

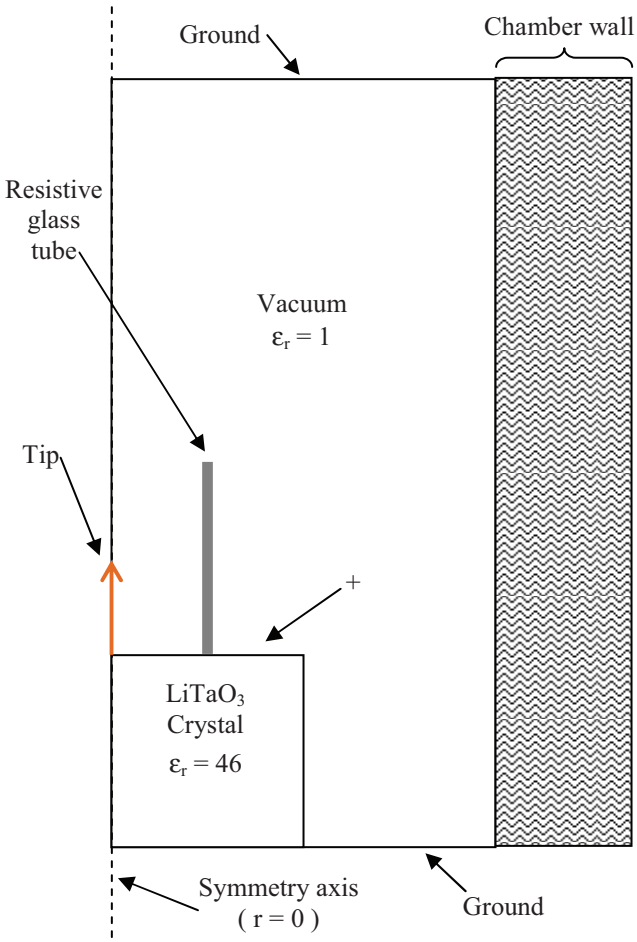

Fig. 3a. Geometry used in COMSOL to represent the system. The axial symmetry of our system was exploited by COMSOL; therefore only half of a cross-sectional view of the system is needed.

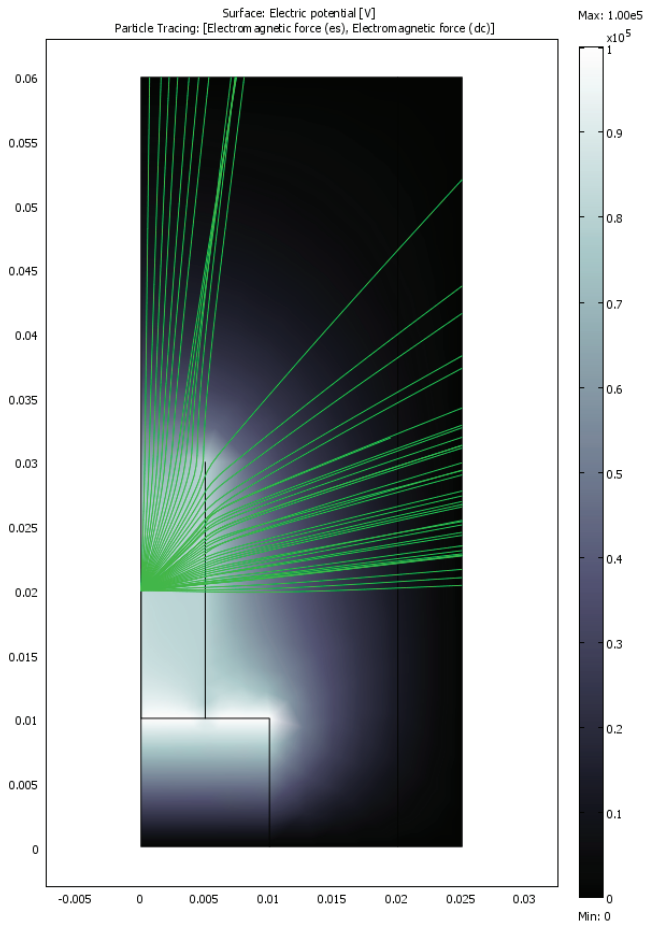

Fig. 3b. COMSOL plot showing the potential distribution (indicated by the background color) and the ion tracks (green lines). Note that the model only considered electrical calculations and therefore did not account for the fact that the ions were not able to penetrate the glass. Consequently, the model shows some ions tracks penetrating the glass tube and striking the chamber wall; these tracks should be disregarded.